

Structural transitions in small molecular clusters

Ana Proykova and Rossen Radev

University of Sofia, Faculty of Physics, Sofia-1126, Bulgaria

Feng-Yin Li

School of Chemical Sciences, University of Illinois, Urbana, Illinois 61801

R. Stephen Berry

Department of Chemistry, The University of Chicago, Chicago, Illinois 60637

(Received 13 August 1998; accepted 12 November 1998)

Clusters of octahedral molecules mimicking TeF_6 afford a vehicle to investigate the analog in small clusters of structural phase transitions through molecular dynamics simulations. Three phaselike forms occur for the solid clusters, both closed-shell structures of 51, 89, and 137 molecules, and open-shell structures of 50, 81, and 129 molecules. The indications are that the free energy has at least two minima as a function of the order parameter. However, whether these converge to a single minimum as N , the number of molecules in the cluster, grows large, leading to a second-order transition in the bulk, or remain apart, implying at least a weak first-order transition in the bulk limit, cannot be determined from the simulations. © 1999 American Institute of Physics.

[S0021-9606(99)51507-9]

I. INTRODUCTION

Structural phase transitions (SPT) in crystals between high-symmetry, disordered and low-symmetry or ordered phases have attracted the attention of both experimentalists and theoreticians for many years.¹ Various anomalies of static and dynamic properties occur in SPT's and have been interpreted within the frameworks of various phase-transition theories. Among the static properties of interest are the temperature dependence of the specific heat and the static dielectric and elastic constants. Experimental techniques such as surface-enhanced Raman scattering and infrared spectroscopy provide realistic information about how these properties change in the transition region.

Structural transformations have been observed in small clusters produced by supersonic nucleation. The experimental conditions for these observations and their analysis can be found in Ref. 2 and the references therein.

The structural phase changes in finite systems may be seen under conditions which, in many cases, have no counterparts for bulk systems.³ Some of the problems of phase behavior of atomic clusters, including surface melting, sintering, phase coexistence, and the passage to the "thermodynamic limit" have been reviewed by Berry and collaborators.⁴⁻⁷ Many clusters have persistent solidlike and liquidlike forms which exhibit a dynamic "solid-liquid" phase equilibrium. That equilibrium becomes a first-order phase transition as N , the number of particles in the cluster, grows very large. This phenomenon is now reasonably well understood.⁷ Some of the phaselike forms of small clusters, such as fluxional structures, disappear as N increases, simply because large systems do not sustain them.

The existence and the nature of a finite-system analog of a second-order phase transition are the subjects that have brought us to the investigation presented previously in Ref. 8 and now here. Many solid bulk systems consisting of highly

symmetrical molecules change their structure at a phase transition as a result of orientation ordering or disordering of the molecules.⁹ Such transitions are usually either second-order or weakly first-order transitions from less ordered to more ordered phases as the temperature is lowered.¹⁰ ("More ordered" is meant in the sense, e.g., free rotation of polyhedral molecules occurs at high temperatures, but does not occur in the form stable at low temperatures).

Many questions arise immediately for the finite system regarding how reordering processes occur, how the free surface of a cluster influences the nature of the reordering phase transition,¹¹ and how finite-size scaling¹²⁻¹⁴ applies for clusters.

In what follows in this article, we attempt to answer some of these questions, while others are discussed elsewhere.^{7,8,11,14-16} The investigation is based largely on simulations of clusters of rigid octahedral molecules intended to mimic TeF_6 . The analysis involves a diagnostic method for extracting the distributions of molecular orientations, which is discussed elsewhere.^{16,17} In Sec. II we describe the procedure used to simulate the dynamics of the molecular clusters in the process of cooling from their melting point and heating from their orientationally ordered phase. In Sec. III, we present the structures and phaselike forms that result from our simulations, and compare the lattice constants computed on the basis of these data with experimental and computational data published by other authors. The visualization is performed with the help of the program XMOL¹⁸ and our animation of the processes.¹⁷ In the final section we discuss the influence of the different factors responsible for the phase changes.

II. SIMULATION PROCEDURE: EXPERIMENTAL AND THEORETICAL BACKGROUND

We have chosen tellurium hexafluoride, TeF_6 , as our model system to answer some of the questions raised in the

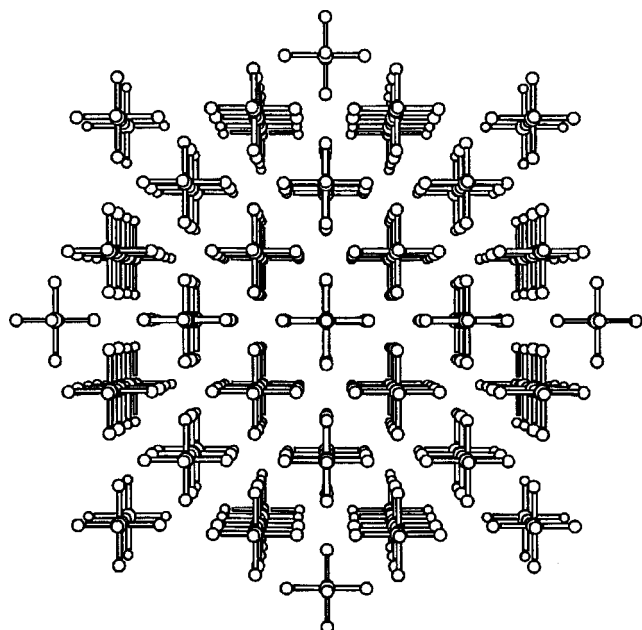


FIG. 1. The initial configuration of a cluster of TeF_6 molecules. The cluster is arranged as spherically as possible with a lattice constant of 6.18 Å, a value obtained from an energy minimization procedure.

Introduction, because the highly symmetrical (octahedral) molecules of TeF_6 provide a good example to study both the nature and the temperature dependence of the structural transformations found in finite molecular clusters. Although TeF_6 is quasispherical in shape, the molecular interaction is sufficiently anisotropic to ensure packing in different crystal structures when the clusters are cooled down from their liquid form. The observations² show a body-centered cubic (bcc) structure below 233 K in the bulk, and, as well, below the melting region for clusters, a monoclinic structure below 100 K and an orthorhombic structure below 50 K. The monoclinic structure has been observed only in clusters, while the others have been found both in clusters and bulk.²

Our simulations, and those performed by Bartell and Xu,¹⁹ indicate that the phase seen below 100 K is stabilized by the kinetics only. We show (Sec. III) that its appearance is a result of partial ordering: only one of the molecular axes of symmetry is aligned.⁸ In addition to the orientation order, a displacive component appears in the simulations. This is detected by the distortions of the lattice even at very low temperatures. Such kinds of distortions are known to be the result of couplings between orientational and translational order in the real system. As the temperature decreases further, the molecules align all their axes with no significant change of the lattice constants.

A. Model for the system and potential function

We describe a cluster of TeF_6 as a classical aggregate of rigid, octahedral species which are allowed to rotate and translate. Initially, the cluster has been arranged as spherical as possible in order to represent the bcc structure found at high temperatures. Technically, this means that a single molecule is located in the cluster center. The first “shell” has eight molecules at the corners of a cube, Fig. 1. The lattice

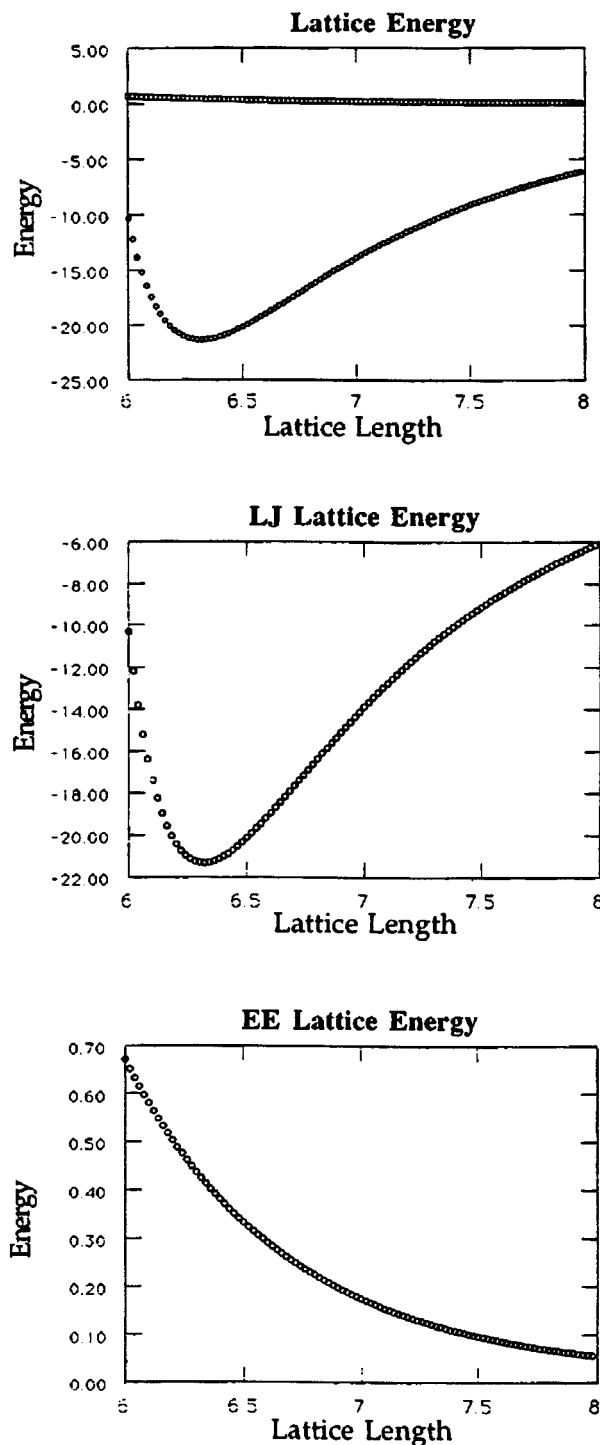


FIG. 2. The minimum value of the total potential corresponding to a lattice constant of 6.18 Å. The value is rather insensitive to the cluster size in the region of configurations studied here.

constant $a = 6.18$ Å is chosen to minimize the potential function, [Eq. (3), below], Fig. 2. The next six molecules belong to the second shell and are located at distance a from the central molecule. In such a way, what is called “shell” hereafter corresponds to a sphere containing a specific number of molecules. For example, in the bcc structure, the first shell contains 9 molecules—1 central and 8 first neighbors. A cluster with two complete shells has 15 molecules—the original 9 plus the 6 of the second shell.

As temperature is reduced, the clusters undergo a structural phase change in the range of a temperature $T_{tr}(N)$ which depends on the cluster size. Our simulations indicate SPT's for clusters of more than about 30 molecules. In order to investigate the influence of possible defects (incomplete shells) on the transformational behavior of the clusters, we have examined a variety of both closed-shell and open-shell structures. For closed-shell bcc structures, we have used 51, 89, and 137 molecules, corresponding, respectively, to 4, 6, and 9 complete shells. For open-shell structures, we have chosen 50, 81, and 129 molecules.

The microscopic state of the cluster is specified in terms of the positions \mathbf{q}_i and momenta \mathbf{p}_i of its constituent set of molecules. These incorporate the orientation degree of freedom. Within the Born–Oppenheimer approximation, it is possible to express the Hamiltonian of the system as a function of the nuclear coordinates and momenta, while the rapid motion of the electrons is averaged to produce the effective potential energy. Additionally, we can assume a classical description of the system and write the Hamiltonian H of the cluster of N molecules as a sum of kinetic and potential energy functions, K and V , respectively, of \mathbf{q}_i and \mathbf{p}_i of each molecule. Adopting the notation $\mathbf{p}=\{\mathbf{p}_i\}$ and $\mathbf{q}=\{\mathbf{q}_i\}$, we have

$$H(\mathbf{p}, \mathbf{q}) = K(\mathbf{p}) + V(\mathbf{q}). \quad (1)$$

Following this model of the cluster, we express the kinetic energy as a sum of translational and rotational motion of each molecule, considered as a rigid polyhedral body,

$$K(\mathbf{p}) = \sum_{i=1}^N 0.5(m_i v_i^2 + \hat{I} \omega_i^2), \quad (2)$$

where m_i is the molecular mass, and \hat{I} is the inertial tensor of a molecule computed in a system fixed with respect to the molecule, where the tensor \hat{I} is diagonal. Its diagonal elements have the same value due to the octahedral symmetry of the molecule, $I_{\alpha\alpha} = I$, $\alpha = 1, 2, 3$.

The potential energy contains the information expressing the intermolecular interactions. The potential function of the system is a sum of pairwise Lennard-Jones atom–atom potentials and an atom–atom Coulomb interaction,

$$V(\mathbf{q}) = \sum_{i < j} U(r_{ij}) = \sum_{i < j} \sum_{\alpha, \beta} \{4\varepsilon_{\alpha\beta} [(\sigma_{\alpha\beta}/r_{ij})^{12} - (\sigma_{\alpha\beta}/r_{ij})^6] + (q_{i\alpha} q_{j\beta} / r_{ij})\}, \quad (3)$$

where the generalized coordinates \mathbf{q} are replaced with the distance $r_{i,j}$ between the i th and j th atom. The indices α, β denote either a fluorine or a tellurium atom. The values for $\sigma_{\alpha\beta}, \varepsilon_{\alpha\beta}$ are taken from Ref. 15: $\sigma_{\text{Te-Te}} = 4.29$, $\sigma_{\text{Te-F}} = 3.55$, $\sigma_{\text{F-F}} = 2.94$ Å.

The Coulomb term in the potential is included²⁰ to account for the observations⁹ that most of the molecular crystals behave as ionic crystals. We have computed the charges $q_{i\alpha}$ with the help of a linear combination of atomic orbitals (LCAO) code in which spherically symmetrical orbital functions are used. The negative charge at the position for any fluorine atom in the molecule is $0.1e$ in this approximation. More sophisticated calculations would give a higher value

for the charges, of the order of $0.25e$ which, however, does not essentially change the relative contribution of the Coulomb potential to the total energy. Because of the higher symmetry of the molecules, the first nonvanishing moment is the hexadecapole. The induced multipoles are negligibly small for this system. The site–site distances for the electrostatic interactions are taken to be the same as those used in the Lennard-Jones potential terms; that is, the charges are placed at the atomic centers.

The potential function (3) accounts for the spatial anisotropy of the molecular interactions which is responsible for the variety of phases exhibited by solid TeF_6 .

The classical equations of motion for a cluster of N molecules interacting via the potential (3) are written in Hamiltonian form. Computing center-of-mass trajectories requires solving a set of $6N$ first-order differential equations. The general requirement is that the Hamiltonian should be independent of the choice of the generalized coordinates in order that the generalized momenta be conserved. For each cluster, as for any set of particles, it is possible to choose six generalized coordinates corresponding to three degrees of freedom of translation of the center of mass, and three independent rotations about the center of mass. The other $(6N-6)$ coordinates describe the motion of the molecules relative to one another. For our case, the potential function depends only on the magnitudes of molecular separation, and V , H , and K are independent of the six translational and orientation coordinates of the entire cluster. The corresponding conjugate momenta, in the Cartesian coordinates, are the total linear momentum

$$\mathbf{P} = \sum_i \mathbf{p}_i$$

and the total angular momentum

$$\mathbf{L} = \sum_i \mathbf{r}_i \times \mathbf{p}_i,$$

where we take the origin of the space coordinate system at the center of mass of the cluster. Having in mind that the cluster is a compound system, we can decompose its angular momentum in two parts,

$$\mathbf{L} = \text{const} = \mathbf{L}_{\text{cluster}} + \sum_j (\hat{I} \cdot \boldsymbol{\omega}_j^b)^s, \quad (4)$$

where $\mathbf{L}_{\text{cluster}}$ is the momentum of the cluster as a whole, and

$$\sum_j (\hat{I} \cdot \boldsymbol{\omega}_j^b)^s$$

is the sum of the individual molecular momenta $\hat{I} \cdot \boldsymbol{\omega}_j^b$ calculated in the body system and projected into the space system. The body system of each molecule has its origin at the center of mass of that molecule. This decomposition allows the decoupling of the motion of the cluster as a whole from the collective motion of the molecules that becomes coherent during the phase transition and leads to alignment of the molecular axes.⁸ Conversions from the body-fixed to space-fixed systems is handled by the equation²¹

$$\omega^2 = \hat{A} \omega^b, \quad (5)$$

where \hat{A} denotes the rotational matrix expressed in terms of quaternions. To complete the picture, we need an equation of motion of the molecular orientation itself. This equation may be replaced by three equations of motions of the Euler angles, or by the four equations for quaternions (q_0, q_1, q_2, q_3) suggested by Evans²² to solve the problem of divergence in the orientation equations for the three Euler angles.

The equations of motions were integrated using the velocity Verlet algorithm.²³ The time step used in our computations was chosen to approximate conservation of energy, linear momentum, and angular momentum adequately. The performance of the algorithm for different time steps Δt in the region of 1 and 30 fs was measured by calculating the root-mean-square energy fluctuations $\langle \delta E^2 \rangle^{1/2} / \langle E \rangle$. At the shortest Δt (1 fs), this was 10^{-7} for a run of 10^5 time steps, and 10^{-5} for a time step of 10 fs. The step of 10 fs was chosen for efficiency.

The boundaries of the clusters were taken free, since no detectable evaporation occurred under the conditions of these simulations. This means, however, that because of the free surfaces of the clusters, the behavior of any local quantity should be specified with care. This is particularly important for any local order parameter which plays a central role in the description of phase transitions. The free surface implies that the order parameter $\xi(\mathbf{r})$ satisfies

$$\xi(\mathbf{r}) = 0 \quad \text{for } |\mathbf{r}| > L, \quad (6)$$

where L is the average linear size of the cluster.

The information about the dynamics of the SPT's of clusters cooled down from their melts is obtained from constant-energy molecular dynamics (MD) simulations. The temperature T of the system is estimated via the average kinetic energy

$$T = \frac{2 \langle E_{\text{kin}} \rangle}{6k_B(N-1)}, \quad (7)$$

where $\langle \rangle$ denotes an average over the trajectory of the cluster in the phase space; k_B is the Boltzmann constant. It is useful to define separate "translational" and "rotational" temperatures, each of which, when averaged, gives T . In such a way we can control the duration of the time t_{eq} necessary for the system to reach a specific temperature

$$\langle E_{\text{kin}}^{\text{rot}} \rangle_{t=t_{\text{eq}}} \cup \langle E_{\text{kin}}^{\text{tr}} \rangle_{t=t_{\text{eq}}}. \quad (8)$$

If the system is far from equilibrium, these two temperatures fluctuate considerably as well as drift toward an equilibrium value.

The cluster is thermalized at a particular temperature using the velocity scaling algorithm

$$\begin{aligned} \sum_i 0.5m_i [\mathbf{v}_i^*(t + \Delta t/2)]^2 &= s^2 \sum_i 0.5m_i [\mathbf{v}_i(t + \Delta t/2)]^2 \\ &= 6Nk_B T. \end{aligned} \quad (9)$$

This velocity scaling procedure has been proven to give the correct canonical distribution in the coordinate space with

accuracy of order Δt if the scaling is carried out in every time step during the thermalization.²⁴ The time necessary to thermalize the cluster if it is far from the transition temperature, which depends on the cluster size, is about 10 ps if the cluster is cooled or heated in steps of 10 K. The closer the temperature is to the transitional range, the longer the thermal equilibration time. Thermal equilibrium is achieved after 100 ps in the vicinity of transition. After the stage of thermal equilibration, the velocity scaling is switched off, and the cluster evolves in the phase space under the condition of constant total energy. It is necessary to run the simulations longer in the transition temperature region than far from it, so the system can come to equilibrium at the new state point. At the end of this equilibrating period, all memory of the initial configuration should have been lost. The system's equilibration is monitored by recording instantaneous values of the potential and kinetic energy during this period. These are taken every ten time steps, i.e., every 0.1 ps, in order to avoid collecting correlated values of the quantities. Adequate equilibration is especially important when the initial configuration is a lattice with one type of symmetry and the state point of interest is in another type of symmetry.

A number of parameters have been monitored to track the changes in the cluster lattice. The degree of translational order in the centers of molecular mass is tested by evaluating the translational order parameter

$$\xi(\mathbf{k}) = \frac{1}{N} \sum_i^N \cos(\mathbf{k} \cdot \mathbf{r}_i),$$

where \mathbf{r}_i is the position vector of the center of mass of the i -th molecule and \mathbf{k} is the reciprocal lattice for the initial lattice. It is found²⁰ that this parameter is a more sensitive indicator of the changes of the lattice structure, and of what constitutes an adequate equilibration period, than the thermodynamic quantities, either V or E_{kin} . The parameter $\xi(\mathbf{k})$ indicates when equilibrium has been reached by converging to a limiting value. In this way we have found that the clusters must equilibrate about 50 ps if they are away from the transition temperature range, and about 1 ns in the range of the transition temperature.

III. RESULTS FOR STRUCTURAL TRANSFORMATIONS AND LATTICE CONSTANTS

Isoenergetic molecular dynamics simulations show that at low temperatures, below $T=20$ K, the clusters are both orientationally and translationally ordered. The program XMOL is used to visualize and plot the structures found in our simulations. We have developed a procedure to extract the lattice constants from the data. Examples of the structure seen at low temperatures in the clusters of 89 and 137 molecules are shown in Figs. 3(a), 3(b), and 4, respectively. In this temperature range the size of the cluster is not very important; the smaller and larger clusters show the same behavior. As we discuss below, the clusters form either a based-centered monoclinic structure, with molecules at the corners having an orientation different from that of the molecules at the centers of the bases, or two intersecting monoclinic structures. Figure 3(b) shows the two spatial orienta-

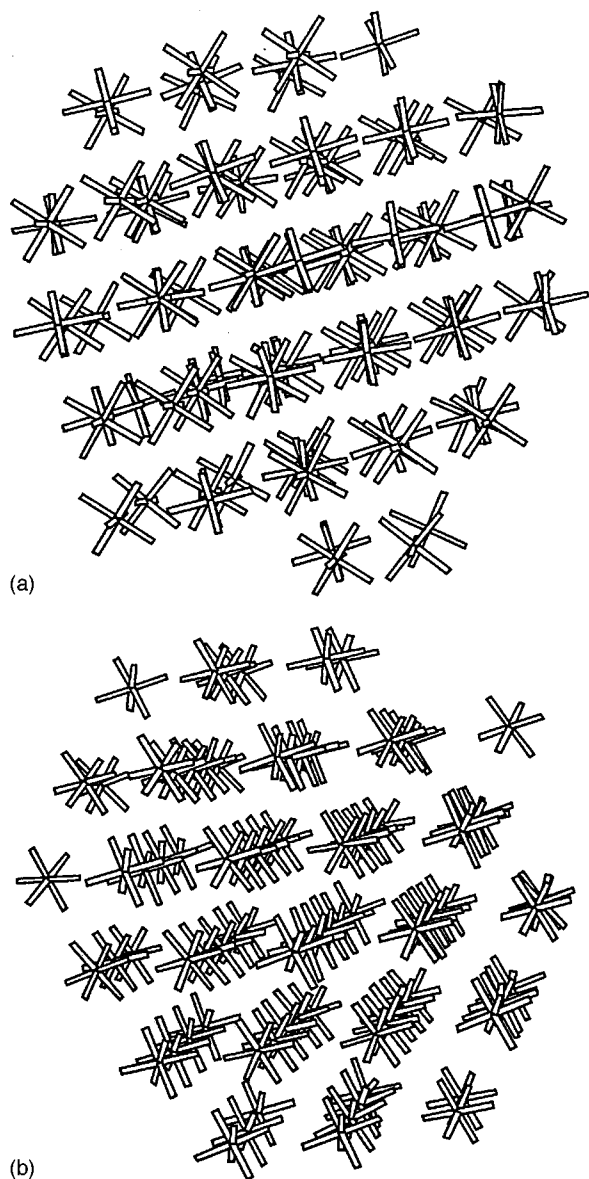


FIG. 3. Two views of the 89-molecule cluster of TeF_6 molecules at 20 K. The figure was produced with the help of XMOL. (a) A view showing how the octahedral molecules are oriented in two specific solid angles; the structure is recognizable as base-centered monoclinic. (b) a view showing that the molecules at the corners have different orientation from those located in the bases.

tions preferred by the molecules. Completely aligned molecules are seen in Fig. 4 for a larger cluster of 137 molecules. Figure 5 illustrates the structure one finds at $T = 20$ K. Only tellurium atoms are shown, and are connected to guide the eye if the distance between them is less than 5.4 Å.

The differences between 89-, 129-, and 137-molecule clusters are apparent in the caloric curves for these three examples, Fig. 6, taken from Ref. 8. The smallest cluster shows the largest, most distinct jump in its caloric curve in the region of the first structural transition. Increasing the size smoothes the jump, indicating that it might exhibit a finite-size effect. In general, this smoothing is not sufficient to assign the transformation as a continuous, second-order transition or as a precursor of such a transition. Additional char-

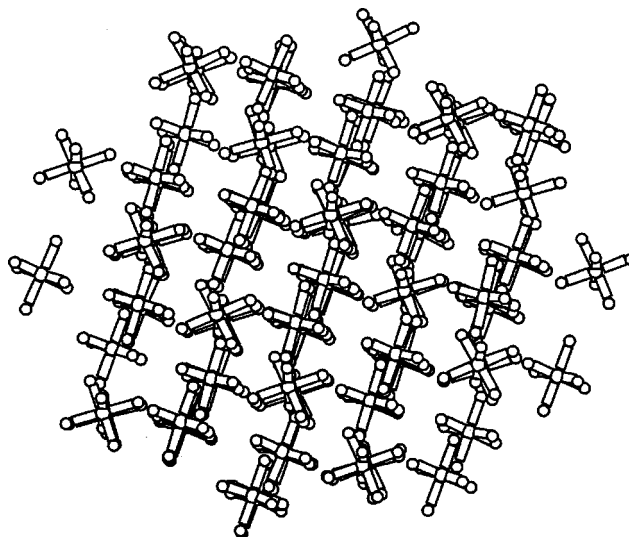


FIG. 4. The 137-molecule cluster of TeF_6 at 20 K. The figure demonstrates that all the molecules, including those on the surface, are aligned in the same orientation.

acteristics of the system should be investigated to make a definite assignment.

We have studied¹⁴ the excess (nonideal) part of the heat capacity, c^{ex} , from the fluctuations of the kinetic energy²⁵

$$\begin{aligned} \frac{1}{N} \langle (\delta E_{\text{kin}})^2 \rangle_{E=\text{const}} &= \frac{3}{2\beta^2} \left(1 - \frac{3}{2c^{\text{ex}}} \right) \\ &= \frac{1}{N} \langle (\delta U_{\text{pot}})^2 \rangle_{E=\text{const}}. \end{aligned} \quad (10)$$

Equation (10) gives the heat capacity per particle and states that the fluctuations of the kinetic and the potential energy are equal and can be verified in a machine computation. The heat capacity shown in Fig. 7 displays the well-

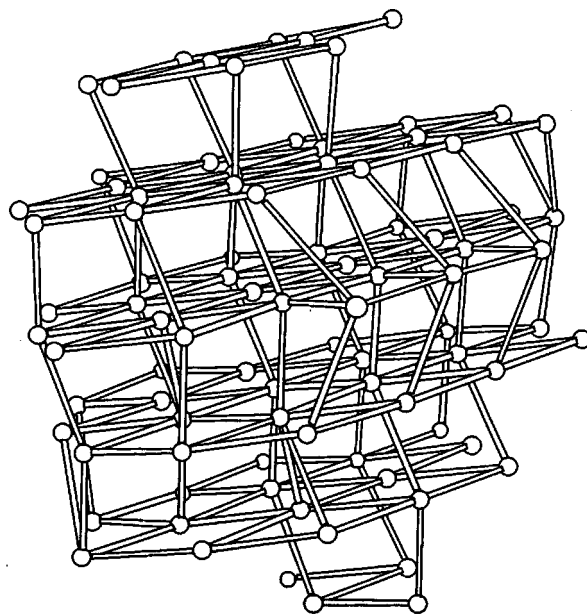


FIG. 5. The lattice structure of a TeF_6 cluster at $T = 20$ K. Only tellurium atoms are shown.

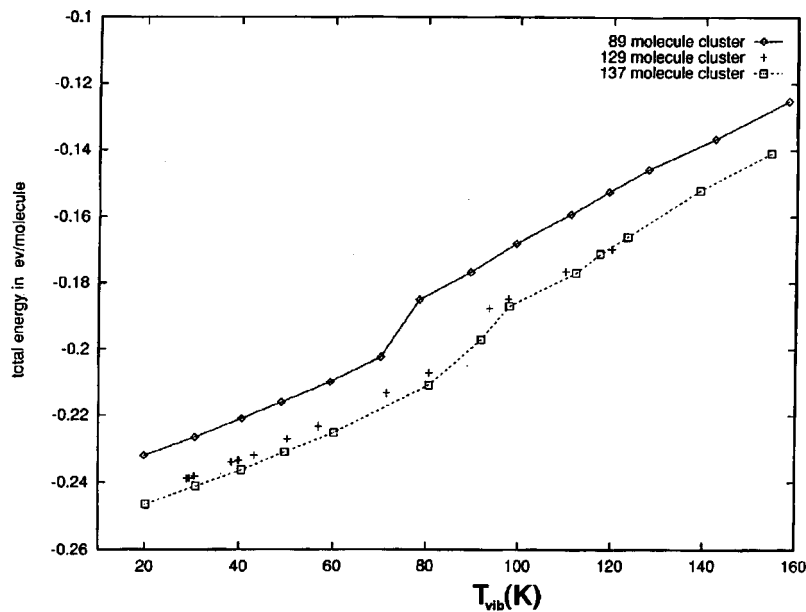


FIG. 6. Caloric curves for the 89-, 129-, and 137-molecule clusters of TeF_6 . The increase of the cluster size causes a smoothing of the jump in the transition temperature region, indicative (but not conclusive proof) of a continuous phase change.

known lambda-type shape as a function of the average temperature [Eq. (7)]. The example of that figure is an 89-molecule cluster heated from $T=20$ in steps of 10 K (5 K in the transition region) up to 160 K. The very large jump at $T=70$ K indicates both orientational and translational changes. On the cooling branch this process goes smoothly, Fig. 7(b). Note that the scales of the two figures differ.

We have determined the orientation distribution of the molecules as functions of cluster size and temperature, to give a clearer guide to this characterization. Here we present the distribution of one of the axes of symmetry relative to one of the space axes,

$$\theta = \arccos[2(q_0^2 + q_3^2) - 1].$$

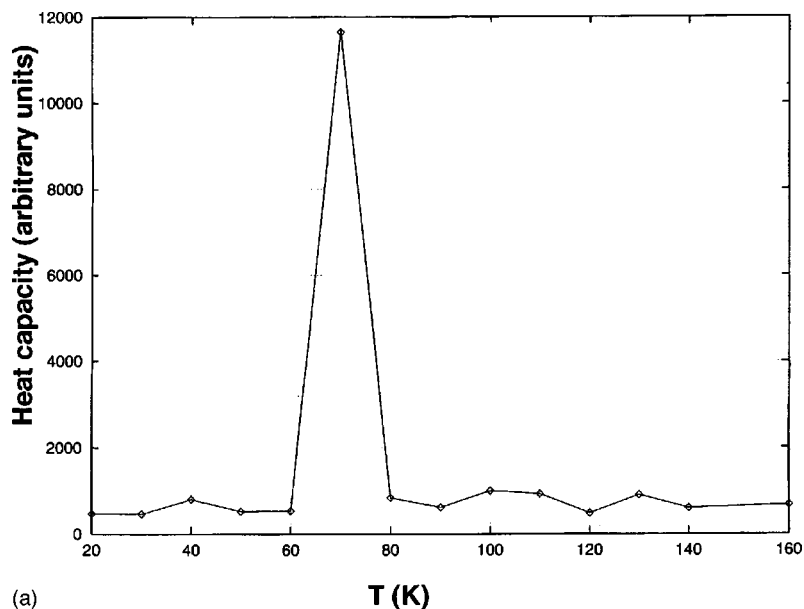
The angular distribution $p(\theta, T)$ is plotted in Fig. 8(a) for the case of a 137-molecule cluster at three different temperatures: $T=180, 80, 20$ K. At high temperatures, all orientations are equally populated, while at and below the transition temperature ($T_c \sim 85$ K for this cluster size) there are two peaks in the angular distribution. The reorientation of the molecules is accompanied by a lattice distortion, as we have seen from the heat capacity curve. At $T=20$ K, the peaks are narrower; the peak at 0 appears to split into two parts because of the symmetry of the molecule: rotation by $\pi/2$ leaves a molecule invariant. A comparison of the distributions at $T=40$ K (just above the second transformation) and $T=20$ K (below it) shows that this transformation does not change the form of the distribution. In order to evaluate the entropy change in this distribution, let us enumerate the microstates.

We denote the number of molecules in the first and second peaks by n_1 and n_2 , respectively. The number of molecules, mostly from the surface, which do not contribute to either peak is n_s : $n_1 + n_2 + n_s = N$, the total number of molecules in the cluster. If all possible permutations of the molecules were allowed, there would be $W = N!/n_1!n_2!n_s!$ different ways in which the specific microstate can be realized. However, Fig. 4 makes it clear that $n_1 = n_2$ when N grows

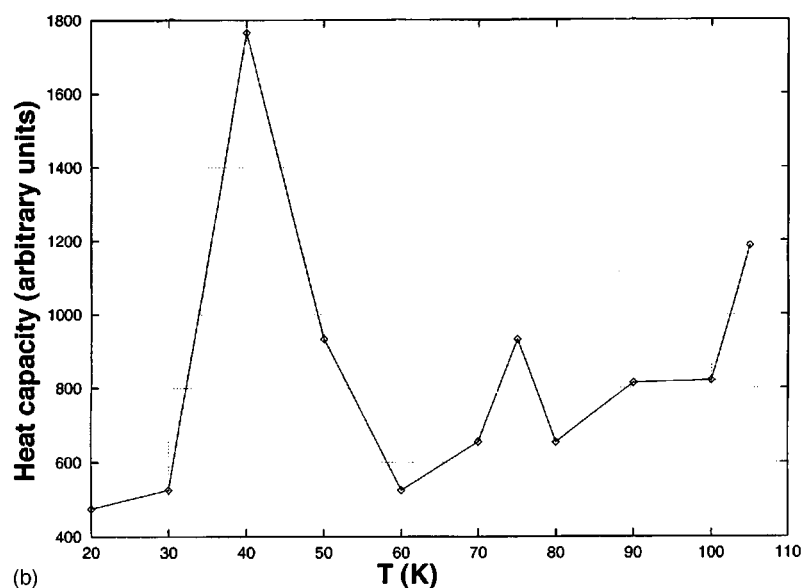
very large. On the other hand, n_s goes to zero as $N^{-2/3}$. Thus the number of states is $W = N!/n_1!N - n_1!$ because $n_2 = N - n_1$. The orientational order, indicated in Figs. 3 and 4, imposes the condition that the orientation of one particle cannot change without changing the orientation of its nearest neighbors, which would induce a change of the next-nearest neighbors, etc. This cannot occur at low temperatures because the system has insufficient energy. As a result, the molecules only librate, as their velocity correlation functions show.¹¹ This is why only exchanges like $n_1 \cap n_2$ can occur. Such exchanges, however, do not change the entropy of the system; this is a strong indication that the phase change is continuous. In smaller systems, the change of the entropy is a smooth process, since it is a finite derivative of the free energy, again consistent with the transition being continuous. This is manifested in the gradual curvature of the caloric curve for the larger clusters at about 30 and about 80 K.

Typical forms of the 89-molecule cluster at 160 and 90 K are shown in Figs. 9(a)–9(c). At 160 K, Fig. 9(a), the cluster has melted: no translational or orientational order is detectable. However, if incidentally one of the molecules evaporates, Fig. 9(b), the cluster cools and spontaneously transforms into a bcc structure. Simulations performed at a constant total energy show such a process clearly. At the temperature of 90 K reached in a cooling process through steps of 10 K (5 K in the transition region), most of the molecules are translationally ordered in a structure distorted because of its finite size; nonetheless they are randomly oriented, Fig. 9(c). Note that the central part of the cluster has a pattern like that produced by bulk crystal growth with defects.

At 80 K, the transition temperature for this cluster size, most of the molecules have aligned one of their symmetry axes, Ref. 8. In the solid–solid transformation detected at 80 K, the crystalline structure (bcc) of the disordered phase collapses due to vibrational modes. At T_c , the amplitudes of some of the slow lattice vibrations become excessively large



(a)



(b)

FIG. 7. The heat capacity calculated from the kinetic energy fluctuations in a 137-molecule cluster: (a) heating; (b) cooling.

for energetic reasons and produce permanent atomic displacements that generate the new crystalline structure as the former becomes unstable. In this case, the measured displacement amplitude is the proper order parameter, $\xi(k)$. Structural transitions that are accompanied by coupling between the rotational and vibrational modes sometimes look like first-order transitions. The free energy has two local minima corresponding to different locally stable population distributions among the uncoupled modes.

This partially ordered structure is not seen in the bulk. In principle, this structure might be only metastable for large systems, stabilized in the small systems by the kinetics and by the stability of coexistence of multiple phaselike (or isomeric) forms with not-too-different free energies. Its consistent appearance in the simulations makes it very likely that it is locally stable up to quite large sizes, perhaps even to the bulk limit. Although it may never be the structure of lowest free energy, it has a free energy close enough to that of other structures that in the dynamic phase equilibrium of an en-

semble of clusters, it is well-populated enough to be important as an equilibrium component.

A further decrease of the temperature causes a complete ordering of all the molecular axes. In infinite systems, complete ordering is achieved in one transformation, with no appearance of the intermediate phase.

If we are to formulate a phenomenological description of dynamics, we must identify a few slow modes whose relaxation times go to infinity at the critical point T_c . Some of these modes interact on a wavelength scale comparable to the coherence length, which diverges in bulk systems. In a finite-size cluster, this length is limited by the linear size. Some of these nonlinear interactions are dissipative and are responsible for the fact that the rates of several irreversible transport processes approach zero at T_c .

To study quantitatively the distributions of molecular orientations, we devised a mapping procedure¹⁶ which makes it easy to determine the relative population of the two preferred orientations denoted by the solid angles Ω_1 and Ω_2 .

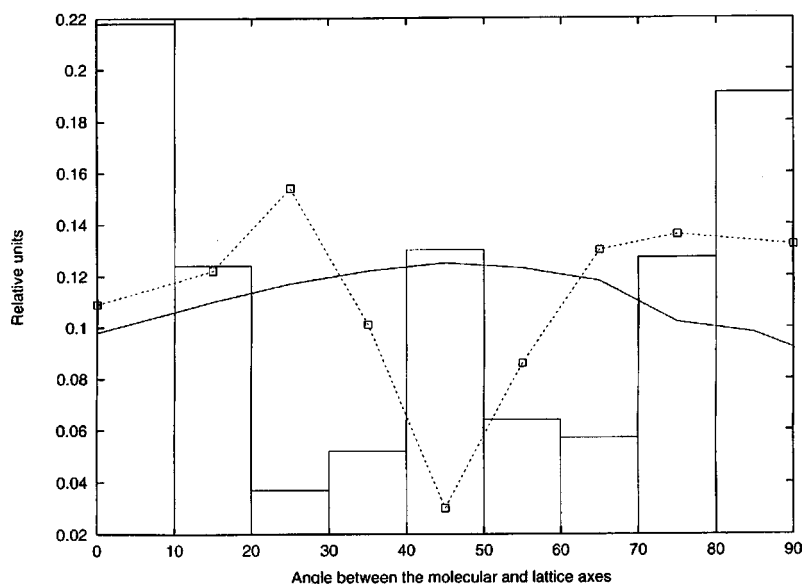


FIG. 8. The distribution of the molecular orientations of the molecules of $(\text{TeF}_6)_{137}$ as a function of temperature. The origin of the coordinate system is at the center of the cluster. The solid curve corresponds to 180 K, the dashed curve to 80 K, and the histogram to 20 K.

Let $N(\Omega_i)$ be the number of molecules oriented in the solid angle Ω_i ; $\sum N(\Omega_i) = N$ is the total number of the molecules in the cluster. Then $p_i = N(\Omega_i)/N$ is the relative population in the direction i . At high temperatures the molecules are oriented randomly and p_i is the same for any direction in the space. At very low temperatures, because of the complete ordering of the molecules, all p_i are zero, with the exception of p_1 and p_2 . The elementary cell of a base-centered monoclinic lattice contains two molecules oriented differently. This means that $p_1 = p_2 = 0.5$ for large clusters of several thousand molecules and for the bulk solid. Clusters of several tens or hundreds of molecules might have p_1 different from p_2 because the number of elementary cells is finite. The sum $S = (p_1 + p_2)$ can be considered as a structural order parameter. It equals 1 in the orientationally ordered phase, and goes continuously to zero as $2/N$ in the disordered phase.

Figure 9(b) shows that the clusters freeze in a slightly distorted, base-centered monoclinic lattice. Such a lattice has an elementary cell consisting of two molecules with random orientations.

We have obtained the following lattice constants: $a = (5.00 \pm 0.06) \cdot 10^{-10}$ m; $b = (5.2 \pm 0.25) \cdot 10^{-10}$ m; $c = (8.7 \pm 0.5) \cdot 10^{-10}$ m and the corresponding angles between the edges: 85, 90, 56°. The crystal structure seen in the clusters is not perfect, even at low temperatures, because of the finite size of these systems, and the consequent influence of their surfaces.

Another interpretation is consistent with the patterns in Figs. 3(a), 3(b), and 4: the lattice can be identified as a combination of two monoclinic structures, since the molecules located in the base center have orientations different from those of the molecules at the corners. This ambiguity of the patterns most probably is the reason for different identifications reported for these structures in the literature. We would like to mention that the static interaction potential is minimized when the molecules oriented in the direction Ω_2 are surrounded by molecules oriented in Ω_1 .

A discussion of the observations and identifications of

the phases in clusters produced in supersonic nucleation can be found in Ref. 2 and references therein. The analysis discussed in these publications is restricted to the experimental data obtained by electron diffraction, which is not sensitive to the molecular orientation. To distinguish between the different molecular orientations, it will be necessary to study the clusters by Raman or infrared spectroscopy.

A recent report²⁶ describes structural phase changes in gold clusters. Whether this sort of transition of atomic clusters is related to those associated with the orientational order-disorder of the molecular clusters studied here is an open issue for the future.

IV. CONCLUSIONS

Structural phase changes as functions of the temperature of clusters of rigid octahedral molecules intended to mimic TeF_6 are inferred from the data computed with the help of constant-energy molecular dynamics simulations. The transformations between different solid structures can be identified as a precursor of the second-order phase transitions in finite systems. The analysis is based on the behavior of the orientational order parameter as a function of the temperature, the heat capacity, and the caloric curve as a function of cluster size. When the temperature is lowered, the cubic lattice undergoes a transition to a (distorted) base-centered monoclinic lattice, i.e., the symmetry is broken. Since the symmetry characters in the two differently oriented lattices are closely related, we can infer from our study that the transformation observed is a two-stage continuous transition. The two transitions differ insofar as one has only a single minimum in the free energy with respect to the order parameter, while the other appears to have two minima which converge as the cluster size increases. This implies that there may be two kinds of bulk second-order transitions, corresponding to these two situations, and that the latter should correspond to borderline cases between weak first-order and true second-order transitions, depending on whether the two

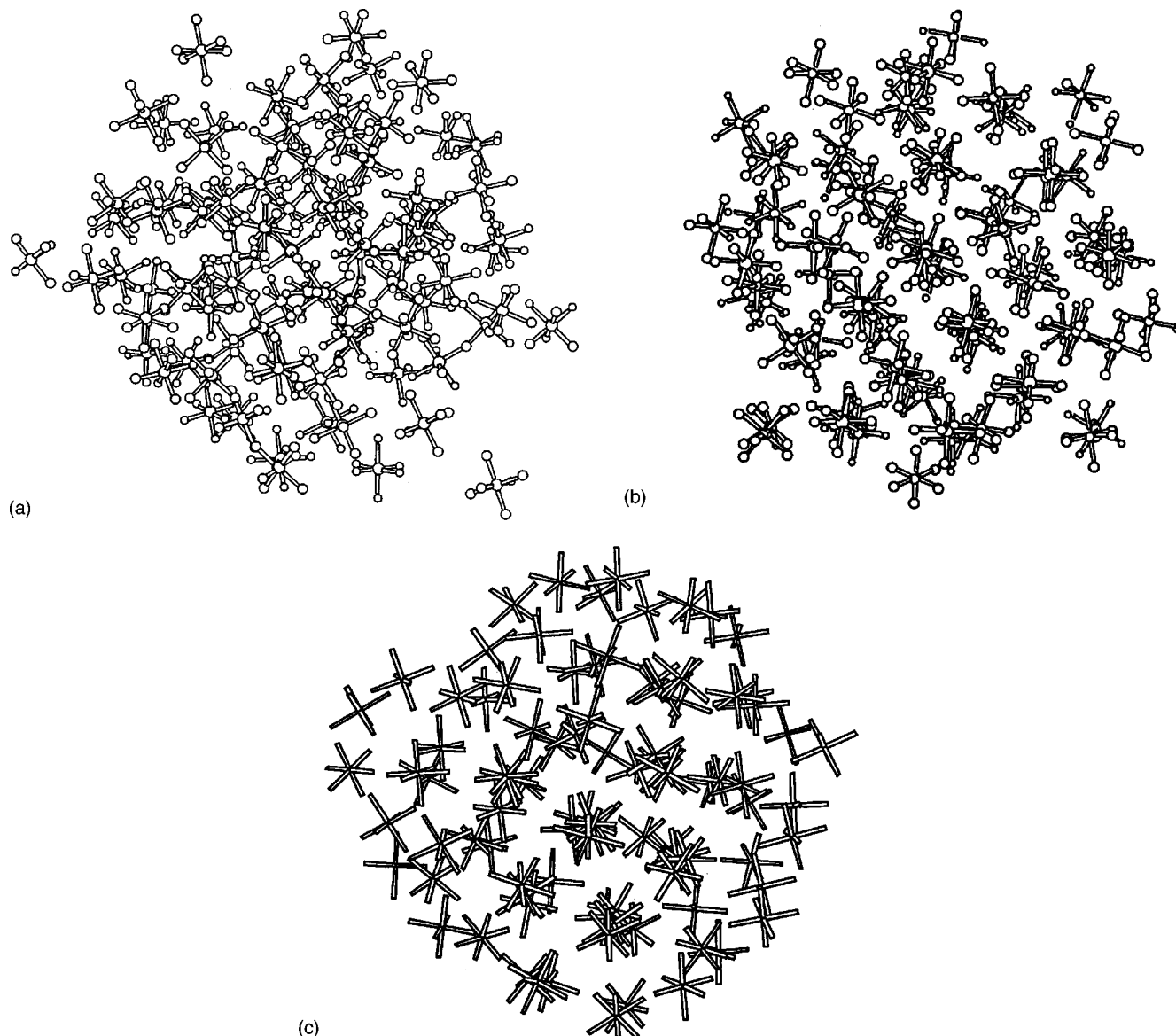


FIG. 9. The 89-molecule cluster of TeF_6 at: (a) 160 K; (b) 160 K—after evaporation of one molecule; (c) 90 K.

minima truly converge at some finite size, converge at infinite size, approach asymptotically but closely enough that the zero-point vibrational level is above the barrier between the minima, or only approach closely enough to leave some small remnant of a latent heat and a double minimum.

ACKNOWLEDGMENTS

A.P. would like to thank the Fulbright Commission for a Fellowship under which much of this work was carried out. R.R. was partially supported by Grant No. 3164/1996 of the Foundation “Scientific Research” of the University of Sofia. The research has been supported by the National Science Foundation Grant No. CHE 9414258.

¹J. F. Scott, *Rev. Mod. Phys.* **46**, 83 (1974).

²L. S. Bartell, E. Valente, and J. C. Calliat, *J. Phys. Chem.* **91**, 2498 (1987).

³R. S. Berry, in *Large Finite Systems*, edited by J. Jortner, A. Pullman, and B. Pullman, The Jerusalem Symposia on Quantum Chemistry and Biochemistry (Reidel, Dordrecht, 1987), Vol. 20.

⁴R. S. Berry, T. L. Beck, H. L. Davis, and J. Jellinek, *Adv. Chem. Phys.* **LXX**, 75 (1988).

⁵F. Amar, J. Bernholc, R. S. Berry, J. Jellinek, and P. Salamon, *J. Appl. Phys.* **65**, 3219 (1989).

⁶R. S. Berry, Hai-Ping Cheng, and J. Rose, in *On Clusters and Clustering—From Atoms to Fractals*, edited by P. J. Reynolds, H. E. Stanley, and E. Guyon (North Holland, Amsterdam, 1993), pp. 227–242.

⁷R. E. Kunz and R. S. Berry, *Phys. Rev. E* **49**, 1895 (1994).

⁸A. Proykova and R. S. Berry, Book of Abstracts of ISSPIC-8, June 29–July 6, 1996, Copenhagen, Denmark; *Z. Phys. D* **40**, 215 (1997).

⁹F. Seitz, *Modern Theory of Solids* (McGraw-Hill, New York, 1940).

¹⁰M. Ferrario, *Computer Simulation in Material Science* (Kluwer Academic, The Netherlands, 1991), pp. 381–393.

¹¹A. Proykova and R. S. Berry, Book of Abstracts of ISSPIC-9 (1998).

¹²M. E. Fisher and V. Privman, *Phys. Rev. B* **32**, 447 (1985).

¹³K. Binder, in *Critical Behavior at Surfaces in Phase Transitions and Critical Phenomena*, edited by C. Domb and J. L. Lebowitz (Academic, New York, 1983), Vol. 8.

¹⁴A. Proykova and R. S. Berry, Book of Abstracts of ISSPIC-9 (1998).

¹⁵J. P. K. Doye, D. J. Wales, and R. S. Berry, *J. Chem. Phys.* **103**, 4234 (1995).

¹⁶R. A. Radev, A. Proykova, F. Y. Li, and R. S. Berry, in *Book of Abstracts of TAMC2*, September 15–20, Lake Geneva, Wisconsin, 1996; *J. Chem. Phys.* **109**, 3596 (1998).

- ¹⁷R. A. Radev, A. Proykova, and R. S. Berry, *Internet J. Chem.* **1**, Article 36 (1998); URL <http://ijc.chem.niu.edu/articles/1998v1/36/>.
- ¹⁸XMOL, version 1.3.1, Network Computing Services, Inc., Minneapolis, MN (1993).
- ¹⁹L. S. Bartell and S. Xu, *J. Phys. Chem.* **95**, 8939 (1991).
- ²⁰F.-Y. Li, R. S. Berry, and A. Proykova, *Book of Abstracts of MWTCC*, May 12–16, Evanston, IL, 1995.
- ²¹M. P. Allen and D. J. Tildesley, *Computer Simulation of Liquids* (Clarendon, Oxford, 1994).
- ²²D. J. Evans, *Mol. Phys.* **34**, 317 (1977).
- ²³L. Verlet, *Phys. Rev.* **159**, 98 (1967).
- ²⁴S. Nosé, *Prog. Theor. Phys. Suppl.* **103**, 1 (1991).
- ²⁵J. B. Lebowitz, J. K. Percus, and L. Verlet, *Phys. Rev.* **153**, 250 (1967).
- ²⁶C. L. Cleveland, W. D. Luedtke, and U. Landman, *Phys. Rev. Lett.* **81**, 2036 (1998).